Supplementary Information:

Redox evolution and the development of oxygen minimum zones in the Eastern Mediterranean Levantine basin during the early Holocene

Authors: Eleen Zirks, Michael Krom, Gerhard Schmiedl, Timor Katz, Yijun Xiong, Lewis J. Alcott, Simon W. Poulton, Beverly Goodman-Tchernov

Age determination:

For the analysis of foraminifera, about 4 g of dried sediment for each sample was wet sieved at 63 µm, dried at 40°C in the oven, and then dry sieved at 125 µm. Mixed surface-dwelling planktic foraminifera were picked for radiocarbon dating.

Table S 1. Data for EZ17G5 and ME0318 used to reconstruct the age models.

Core name	Core depth (cm)	^{14}C age ± 1σ (kyr BP)	Calendar age ± 2σ (cal. kyr BP)	Measured on
EZ17G5	0		0	Surface sediment
	37-38	3.914 ± 0.031	3.896 ± 0.106	Mixed planktic foraminifera
	80-81	6.174 ± 0.038	6.605 ± 0.110	Mixed planktic foraminifera
	94-95	7.762 ± 0.040	8.239 ± 0.093	Mixed planktic foraminifera
	110-111	8.819 ± 0.041	9.473 ± 0.068	Mixed planktic foraminifera
	216-217	15.277 ± 0.065	18.091 ± 0.197	Mixed planktic foraminifera
ME0318	0		0	Surface sediment
	30-31	2.855 ± 0.037	2.604 ± 0.118	Mixed planktic foraminifera
	86-87	5.711 ± 0.051	6.118 ± 0.134	Mixed planktic foraminifera
	129-130	7.961 ± 0.039	8.430 ± 0.088	Mixed planktic foraminifera
	183-184	12.156 ± 0.058	13.609 ± 0.167	Mixed planktic foraminifera

Precision and accuracy information for the X-ray fluorescence analyses:

Precision and accuracy were determined on each analytical run of the XRF. The Relative Standard Deviation (R.S.D.) was determined by taking the standard deviation obtained from the XRF which scanned a series of areas of a single sample and calculated the average and Std. Dev. of the values. The Std. Dev. was concentration dependent and the values given in this table were from samples with a concentration close to the values used in the depth profiles from the two cores sampled. The accuracy was determined using multiple analytical standards

to create a regression line. In the table we report the number of analytical standards used and the linear regression coefficient of the line obtained.

Table S2:

Table of Performance characteristics for chemical analysis of major and minor elements by X-ray Fluorescence:

Element	Conc. units	R.S.D. calculated from the Std. Dev. x 100/ average concentration of a random sample	Linear regression coefficient (R^2)	Number of analytical standards used per calibration
Al	%	0.6	0.909	6
Ti	%	1.2	0.952	6
Mg	%	1.1	0.987	7
Ca	%	0.5	0.993	6
V	µg/g	3.1	0.981	5
Mn	µg/g	1.6	0.999	6
Ba	µg/g	1.2	0.981	5
U	µg/g	8.8	0.985	3
Mo	µg/g	3.9	0.991	3

Fe and P speciation procedures:

The Fe speciation methods were developed from Poulton and Canfield, 2005 and Canfield et al., 1986, as used by Zegeye et al., 2012, Goldberg et al., 2012 and Xiong et al., 2019. The procedure targets six operationally-defined phases, with steps I-III performed sequentially (for extraction details see Table S3, which also reports target Fe phases and the precision of each extraction based on replicate extractions).

Table S3. Fe extraction protocol. Steps I-III were performed sequentially on a sub-sample, and steps IV and V were performed sequentially on a separate subsample.

Step	Extraction details	Target Fe phases	RSD (%)
I	5 mL 0.5 M HCl (shake for 1h)	**$Fe(II)_{unsulf}$**: Extraction targets reduced solid phase Fe, including AVS and Fe(II) phosphates. Subtraction of Fe_{AVS} (step IV) gives unsulfidized solid phase Fe(II) **Fe_{ox1}**: Extraction also gives total Fe (i.e., Fe(II) + Fe(III)) solubilized by this technique. Subtraction of Fe(II) gives highly reducible ferric oxides such as ferrihydrite	3 11
II	10 mL sodium citrate/acetic acid/sodium dithionite solution (58.82 g/L sodium citrate, 20 mL/L acetic acid, 50 g/L sodium dithionite, shake for 2 h)	**Fe_{ox2}**: Reducible ferric oxides such as goethite and hematite	4
III	10 mL ammonium oxalate/oxalic acid (28.42g/L ammonium oxalate, 21.45 g/L oxalic acid, shake for 6h)	**Fe_{mag}**: Magnetite	5
IV	8 mL 50% HCl (boil for 1h)	**Fe_{AVS}**: Acid volatile sulfide	5
V	5 mL 1M chromous chloride dissolved in 50% HCl (boil for 1 h)	**Fe_{sul}**: Pyrite	5

The sequential extraction method (SEDEX) for different phosphorus phases was modified from Ruttenberg, 1992. Five sedimentary P reservoirs were extracted by different reagents as detailed in Table S4.

Table S4. Sequential SEDEX steps for different target P phases.

Step	Extractant	Target P phase	RSD (%)
I	5 mL 1 M $MgCl_2$ (pH 8, shake for 2h) × 2	**P_{sorb}**: loosely sorbed P	5

	5 mL MilliQ water (shake for 2h) × 2		
II	10 mL sodium citrate/sodium bicarbonate/sodium dithionite solution (88.23 g/L sodium citrate, 84.01 g/L sodium bicarbonate, 24.38 g/L sodium dithionite, shake for 8 h) 5 mL 1 M $MgCl_2$ (pH 8, shake for 2 h) 5 mL MilliQ water (shake for 2 h)	**P_{Fe}**: Fe-bound P	2
III	10 mL, 1 M acetate sodium (pH 4, shake for 6h) 5 mL 1 M $MgCl_2$ (pH 8, shake for 2 h) × 2 5 mL MilliQ water (shake for 2 h)	**P_{auth}**: Carbonate-associated P, authigenic apatite and biogenic apatite	3
IV	10 mL 10% HCl (shake for 16 h)	**P_{detr}**: Detrital apatite and other inorganic P phases	2
V	Ash at 550 ℃ 10 mL 10% HCl (shake for 16 h)	**P_{org}**: Organic phosphorus	3

Use of Benthic foraminifera species to define oxygen status of overlying water:

In these figures benthic foraminifera species can be generally grouped into preferentially epifaunal (green), shallow infaunal (red) and deep infaunal species (blue) for core EZ17G5 (Figure S1), core ME0318 (Figure S2) ands SL112 (Figure S3). These data are used to help interpret the oxygen status of the overlying water.

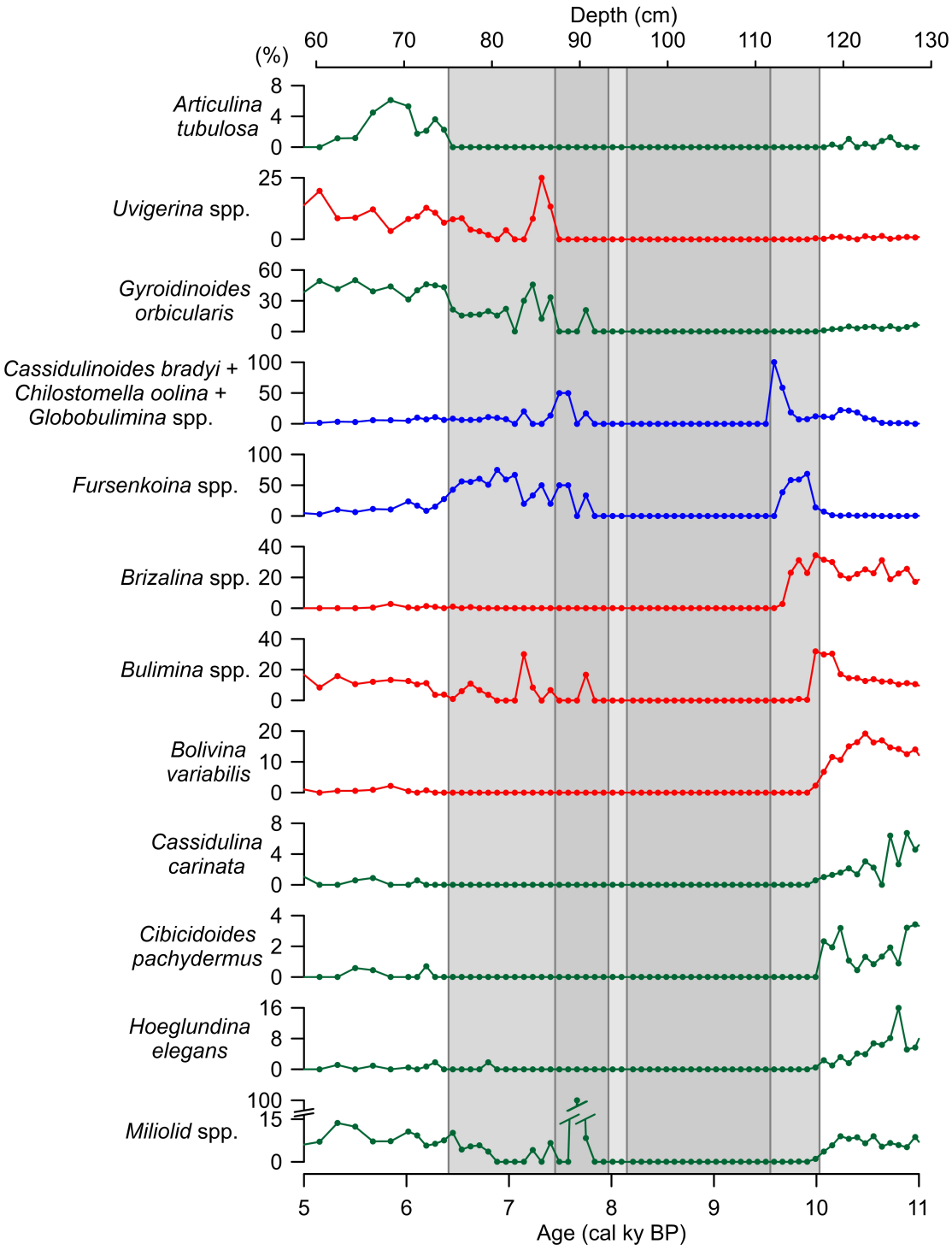

Figure S1: Selected benthic foraminifera species in percent from sediment core EZ17G5. Green indicate epifaunal, red shallow infaunal and blue deep infaunal species. The oxygen status of the overlying water is shown in different shades of grey and defined in Figure 3 legend.

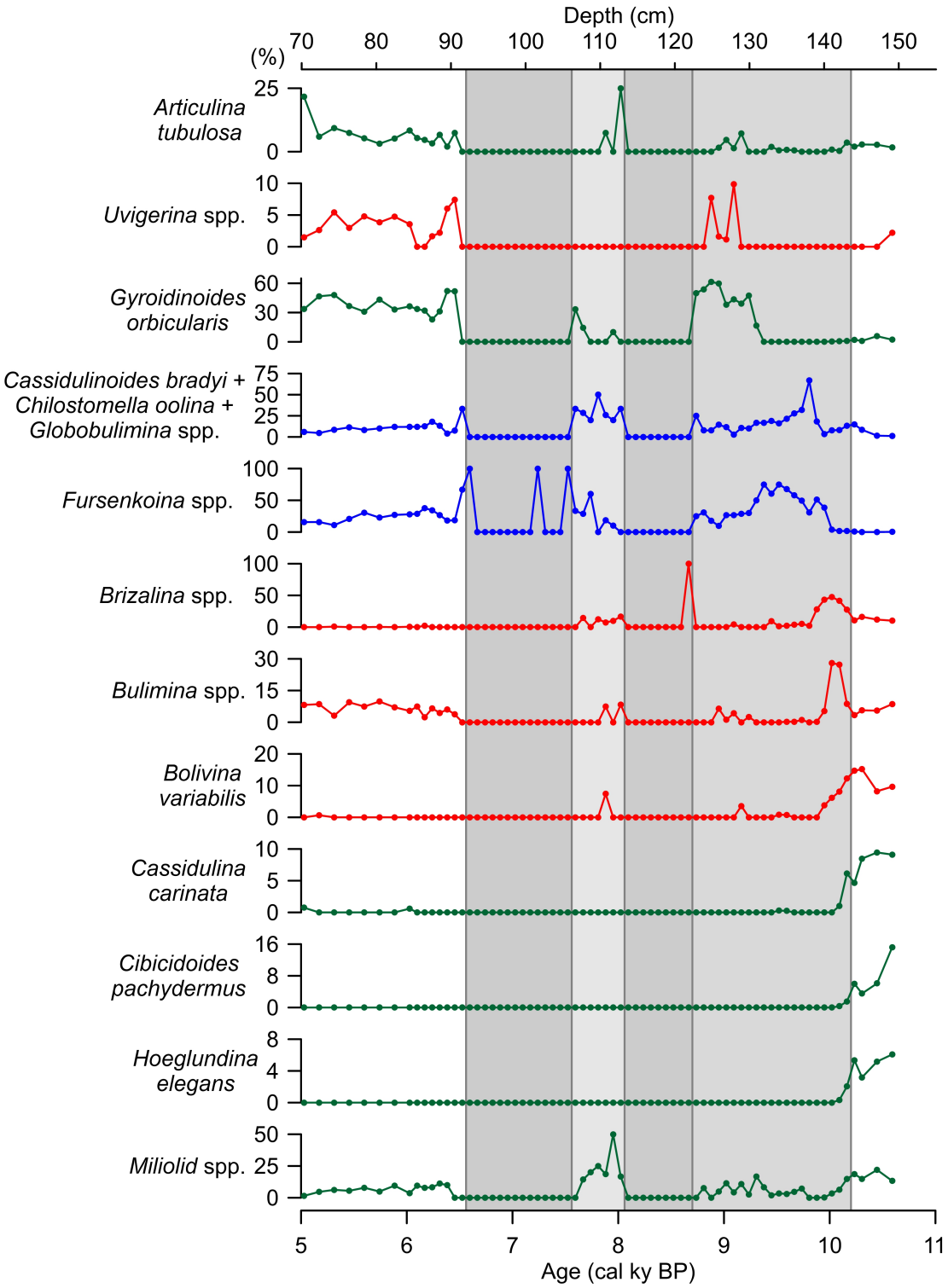

Figure S2: Selected benthic foraminifera species in percent from sediment core ME0318. Green indicate epifaunal, red shallow infaunal and blue deep infaunal species. The oxygen status of the overlying water is shown in different shades of grey and defined in Figure 3 legend.

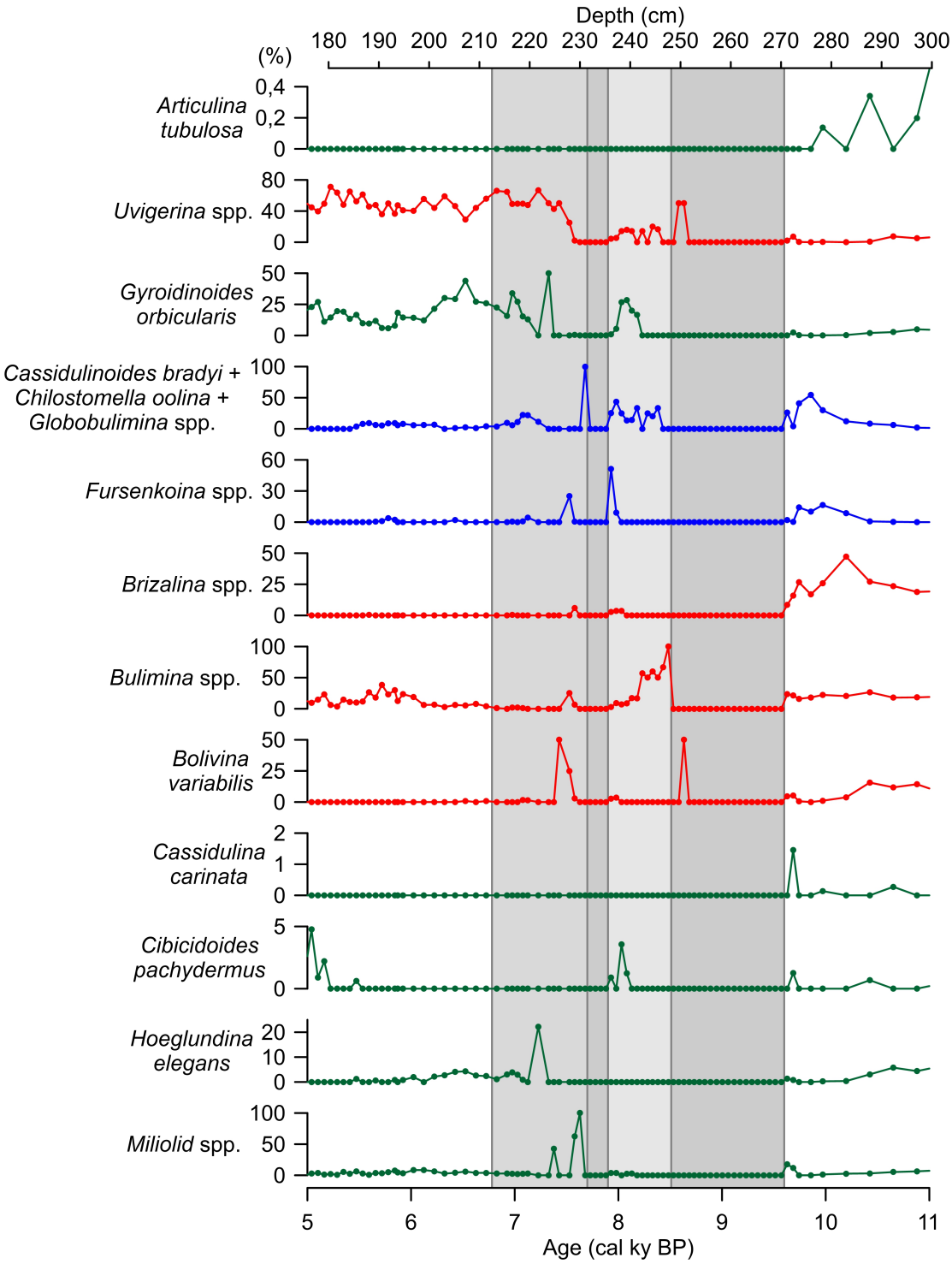

Figure S3: Selected benthic foraminifera species in percent from sediment core SL112 (Kuhnt, 2008). Green indicate epifaunal, red shallow infaunal and blue deep infaunal species. The oxygen status of the overlying water is shown in different shades of grey and defined in Figure 3 legend.

Canfield, D.E., Raiswell, R., Westrich, J.T., Reaves, C.M., Berner, R.A., 1986. The use of chromium reduction in the analysis of reduced inorganic sulfur in sediments and shales. Chem. Geol. 54, 149–155. https://doi.org/http://dx.doi.org/10.1016/0009-2541(86)90078-1

Goldberg, T., Archer, C., Vance, D., Thamdrup, B., McAnena, A., Poulton, S.W., 2012. Controls on Mo isotope fractionations in a Mn-rich anoxic marine sediment, Gullmar Fjord, Sweden. Chem. Geol. 296–297, 73–82. https://doi.org/10.1016/j.chemgeo.2011.12.020

Kuhnt, T., 2008. Reconstruction of Late Quaternary Deep-Sea Ecosystem Variability in the Eastern Mediterranean Sea based on Benthic Foraminiferal Faunas and Stable Isotopes. Universität Leibzig, Germany.

Poulton, S.W., Canfield, D.E., 2005. Development of a sequential extraction procedure for iron: implications for iron partitioning in continentally derived particulates. Chem. Geol. 214, 209–221. https://doi.org/10.1016/j.chemgeo.2004.09.003

Ruttenberg, K.C., 1992. Development of a sequential extraction method for different forms of phosphorus in marine sediments. Limnol. Oceanogr. 37, 1460–1482. https://doi.org/10.4319/lo.1992.37.7.1460

Xiong, Y., Guilbaud, R., Peacock, C.L., Cox, R.P., Canfield, D.E., Krom, M.D., Poulton, S.W., 2019. Phosphorus cycling in Lake Cadagno, Switzerland: A low sulfate euxinic ocean analogue. Geochim. Cosmochim. Acta. https://doi.org/10.1016/j.cois.2017.06.009

Zegeye, A., Bonneville, S., Benning, L.G., Sturm, A., Fowle, D.A., Jones, C., Canfield, D.E., Ruby, C., MacLean, L.C., Nomosatryo, S., Crowe, S.A., Poulton, S.W., 2012. Green rust formation controls nutrient availability in a ferruginous water column. Geology 40, 599–602. https://doi.org/10.1130/G32959.1